Synthesis, characterization and fabrication on a glassy carbon electrode of a tetra-iron substituted sandwich-type pentadecatungstodiarsenate heteropolyanion†

Lihua Bi, Jianyun Liu, Yan Shen, Junguang Jiang and Shaojun Dong*

State Key Laboratory of Electroanalytical Chemistry, Changchun Institute of Applied Chemistry, Chinese Academy of Sciences, Changchun 130022, P. R. China. E-mail: dongsj@ns.ciac.jl.cn; Fax: +86-431-5689711; Tel: +86-431-5262101

Received (in Montpellier, France) 13th June 2002, Accepted 16th December 2002
First published as an Advance Article on the web 26th February 2003

A novel sandwich-type compound, $Na_{12}[Fe_4(H_2O)_2(As_2W_{15}O_{56})_2]\cdot 41H_2O$, has been synthesized. The compound was well-characterized by means of IR, UV-vis, ^{183}W NMR and elemental analyses. The compound crystallizes in the triclinic, $P\bar{1}$ symmetry group. The structure of the compound is similar to that of $Na_{16}[M_4(H_2O)_2(As_2W_{15}O_{56})_2]\cdot nH_2O$ (M = Cu, Zn, Co, Ni, Mn, Cd), and consists of an oxo-aqua tetranuclear iron core, $[Fe^{III}_4O_{14}(H_2O)_2]$, sandwiched by two trivacant α-Wells-Dawson structural moieties, α-$[As_2W_{15}O_{56}]$. Redox electrochemistry of the compound has been studied in buffer solutions at pH = 4.7 using polarography and cyclic voltammetry (CV). The compound exhibited four one-electron couples associated with the Fe(III) center followed by three four-electron redox processes attributed to the tungsten-oxo framework. The compound-containing monolayer and multilayer films have been fabricated on a 4-aminobenzoic acid modified glassy carbon electrode surface by alternating deposition with a quaternized poly(4-vinylpyridine) partially complexed with $[Os(bpy)_2Cl]^{2+/-}$. CV, X-ray photoelectron spectroscopy (XPS), UV-vis spectroscopy and atomic force microscopy (AFM) have been used to characterize the multilayer films. It is proved that the multilayer films are uniform and stable. The electrocatalytic activities of the multilayer films have been investigated on the reduction of two substrates of important analytical interest, NO_2^- and H_2O_2.

Introduction

Polyoxometalates (POMs) are a distinctive class of inorganic metal-oxygen cluster compounds that have found applications in fields as diverse as catalysis, analysis, medicine, biochemistry, material science, and so on.[1–6] Among the large family of POMs, transition metal-substituted POMs (TMSPs) exhibit unique chemical and electrochemical properties. Recently, considerable attention has been directed towards TMSPs.[7–9] The heteropolyanion bears some similarities not only in its coordination environment but also its catalytic reactivity to metalloporphyrins and to other metal complexes of macrocyclic ligands.[10] The heteropolyanion ligands are robust under strongly oxidative conditions and thus have an important advantage over metalloporphyrin systems, which decompose under these conditions.[11]Important properties (acidity, stability and redox potential, *etc.*) of TMSPs can be adjusted by substitution of selected atoms and by the choice of pH range. Consequently, suitable organic catalysis and electrocatalysis may be designed.

Most of the electrochemical investigations of TMSPs have concerned the POM anions having Keggin or Dawson structures.[12–15] Fe(III) substituted POMs are the most popular. Zonnevijlle *et al.* reported the preparation and electrochemical characterization of a Fe(III) Dawson-type POM.[16] Toth, Anson and coworkers investigated the electrochemical properties of a Fe(III)-substituted Keggin-type POM and studied its electrocatalytic properties towards reduction of nitrite or nitric oxide and H_2O_2.[17] Dong and Liu characterized the electrochemical properties of a Fe(III)-substituted Dawson-type POM and found that its electrocatalytic properties were similar to the Fe(III) Keggin case.[18] To our knowledge, electrochemical studies of sandwich-type TMSPs are rare. Recently, Song *et al.*[19a] and Ruhlmann *et al.*[19b] reported an electrochemical study of a sandwich-type TMSP, $Fe_4(H_2O)_2(P_2W_{15}O_{56})_2$, and its ability to reduce NO_2^- and H_2O_2 electrocatalytically in aqueous solution, respectively.[19] The sandwich-type TMSPs are compounds prepared by coordination of two trivacant anions from Keggin or α-Wells–Dawson structural moieties with four M cations. Compounds with P as the heteroatom were previously reported by the groups of Finke,[20–23] Weakley,[23,24] Pope[25] and Coronado[26] and used later in other applications by Gomez-Garcia,[27] Hill[28] and Neumann[29] *et al.* This kind of POM has a large molar mass, higher negative charge and more transition metals, so they have many interesting properties,[30] such as magnetic,[31] good catalytic activity[32] and anti-AIDs activity,[33] *etc.* Recently, Wang and his coworkers reported the preparation, characterization and the replacement reaction of coordinated water molecules of analogous heteropolyanions with As as the heteroatom.[34] In this paper, we report the synthesis, electrochemical behavior and self-assembly of $Na_{12}[Fe_4(H_2O)_2(As_2W_{15}O_{56})_2]$ on glassy carbon electrode surfaces as monolayer and multilayer films of nanoscopic dimensions based on electrostatic interactions.

The layer-by-layer assembly of oppositely charged species has been proven to be a promising method in fabricating uniform and ultrathin film devices at room temperature from aqueous solution.[35–37] It provides a novel route for the formation of various ordered structures at the molecular level.[38,39]

† Electronic supplementary information (ESI) available: model of layer formation, CV of 4-ABA on a GCE and of QPVP-Os/4-ABA/GCE in pH 4.7 buffer, plots of E_d *vs.* log $(i/i_d - i)$ and XRD of the title compound. See http://www.rsc.org/suppdata/nj/b2/b205766m/

 DOI: 10.1039/b205766m

Practical applications of POMs in many areas depend on their successful immobilization.[40] Recently, TMSPs have been organized as multilayer films using the Langmuir–Blodgett technique and they have also found application as the inorganic component of conducting films.[41] The structure of $Na_{12}[Fe_4(H_2O)_2(As_2W_{15}O_{56})_2]$ consists of an oxo-aqua tetranuclear iron core, $[Fe_4^{III}O_{14}(H_2O)_2]$, sandwiched by two trivacant α-$As_2W_{15}O_{56}^{12-}$. The compound has some unusual advantages. For example, (i) it is highly oxidation resistant and thermally robust; (ii) it can work in both polar and non-polar solvents; (iii) it may show rich redox chemistry originating from the well-known addenda atoms (W) as well as the substituted transition metals (Fe), which may function as catalytic active sites; (iv) it is a water-soluble yellow crystal, solutions of which are very stable between pH 1.5 and 6.5. Consequently, $Na_{12}[Fe_4(H_2O)_2(As_2W_{15}O_{56})_2]$ was electrochemically grafted onto the carbon substrate surface by electrostatic interactions. The novel tunable monolayer and multilayer films may find potential applications as diverse as in electrochromism, photoelectrochemistry, sensors, catalysis, light imaging, and other thin-film molecular devices.

Experimental

Materials

Reagents. 4-Aminobenzoic acid (4-ABA) was purchased from Aldrich. The absolute ethanol was dried over 3 Å molecular sieves before use. The solution of 4-ABA was freshly prepared for each modification. Lithium perchlorate was dried at about 90 °C before use. The polycation, quaternized poly-(4-vinylpyridine) partially complexed with $[Os(bpy)_2Cl]^{2+/-}$ (QPVP-Os), was provided by Professor Xi Zhang (Jilin University, China). All of the other chemicals were of reagent grade and used as received. Water used for the preparation of aqueous solutions was purified using a Millipore-Q water purification system. Buffer solutions were prepared from 0.5 M NaAc + HAc (pH = 3–6), 0.5 M $Na_2SO_4 + H_2SO_4$ (pH = 1–3) and 0.1 M $NaH_2PO_4 + Na_2HPO_4$ (pH = 6–9).

Synthesis of $Na_{12}[Fe_4(H_2O)_2(As_2W_{15}O_{56})_2]\cdot 41H_2O$ ($Fe_4As_4W_{30}$). α-$Na_{12}As_2W_{15}O_{56}\cdot 21H_2O$ (As_2W_{15}) was prepared according to the literature method.[34] The title compound was prepared as described previously.[42] The synthetic procedure was as follows: $FeCl_3\cdot 6H_2O$ (0.68 g, 2.49 mmol) was dissolved in 50 mL of a 2 M NaCl solution; solid As_2W_{15} (5.0 g, 1.12 mmol) was then added and dissolved by vigorous stirring. The color of the solution turned from yellow to orange. The solution was heated to 80 °C for 10 min and filtered while hot. The resulting clear orange solution was cooled to 5 °C overnight, from which a yellow solid was then collected. Good quality crystals were obtained by recrystallization of the yellow solid from 20 mL of a 2.0 M NaCl solution. The yield was 3.25 g (65%). Anal. calcd (found) for $Na_{12}As_4W_{30}Fe_4(H_2O)_2O_{11}\cdot 41H_2O$: Na, 3.11 (3.18); As, 3.38 (3.32); W, 62.10 (62.20); Fe, 2.52 (2.58); H_2O, 8.31 (8.42).

Preparation of the $Fe_4As_4W_{30}$-containing monolayer and multilayer films. A schematic illustration of the deposition procedures and conceptual models of the monolayer and multilayer films consisting of POMs and QPVP-Os on the negatively charged precursor 4-ABA are given in the Electronic supplementary information (ESI, S1). The electrochemical modification of a glassy carbon electrode (GCE) was performed according to the published procedures.[43] The cyclic voltammetry (CV) of 3 mM 4-ABA in 0.1 M $LiClO_4$ ethanol solution on a GCE at 10 mV s^{-1} with repeated scanning and the scheme of the oxidation of 4-ABA and grafting on GCE are given in the ESI (S2). The oxidation wave at about +0.73 V is attributed to a one-electron oxidation of the amino group of 4-ABA to its cation radical. By repeated scanning, the peak gradually diminishes, indicating the formation of a coating on the electrode surface.[44]

The 4-ABA/GCE was first placed in QPVP-Os + 0.1 M acetate buffer (pH 3.8) and then scanned between 0.6 and −0.1 V at a scan rate of 100 mV s^{-1} for 25 cycles. The modified electrode with the QPVP-Os layer was then placed in 2.0 mM $Fe_4As_4W_{30}$ + 0.5 M acetate buffer (pH 4.7), resulting in one layer of $Fe_4As_4W_{30}$ by scanning under similar conditions to those used above. When the resulting electrode was placed alternatingly in QPVP-Os and $Fe_4As_4W_{30}$ solutions, $Fe_4As_4W_{30}$ multilayer films were formed. Cyclic potential scanning for 25 cycles proved to be sufficient for loading $Fe_4As_4W_{30}$ and QPVP-Os.

Measurements

Electrochemical. CV was performed with a CHI 600 electrochemical workstation (USA, Shanghai Shenhua instrumental company) in a conventional three-electrode electrochemical cell using glassy carbon (GC 2000, 3 mm diameter, Tokai Corp., Japan) as the working electrode, except for the electrochemical experiment of POM species in aqueous solution, which was done using a glassy carbon electrode of 1 mm diameter. Twisted platinum wire was used as the auxiliary electrode, with a Ag/AgCl reference electrode in aqueous media or a Ag/Ag^+ (0.01 M $AgNO_3$) reference electrode in anhydrous ethanol solutions. The glassy carbon electrodes were successively polished with 1.0 and 0.3 μm α-Al_2O_3 powders and sonicated in water for about 3 min after each polishing step. Finally, the electrodes were sonicated in ethanol, washed with ethanol, and dried with α high purity nitrogen stream immediately before use. The polarography was studied using a 384B polarographic analyzer with a 303A-type electrode.

XPS. XPS measurements were performed on an ESCALAB-MKII spectrometer (VG Co., UK) with Mg Kα radiation as the X-ray source for excitation and an analyzer pass energy of 50 eV. Typically, the operating pressure in the analysis chamber was below 10^{-9} Torr. XPS measurements were performed on glassy carbon plates modified with $Fe_4As_4W_{30}$ multilayer films.

UV-vis. UV-vis absorption spectrometric experiments were carried out with a DMS-90 UV-vis spectrophotometer (Varian Inst. Co., Palo Alto, CA). UV-vis spectra of free QPVP-Os and $Fe_4As_4W_{30}$ were first measured in pH 3.8 0.1 M NaAc + HAc and pH 4.7 0.5 M NaAc + HAc solution in a quartz cuvette to determine a suitable wavelength range for featuring the absorption of the two modifiers. For UV-vis measurements of multilayer films, a quartz slide silanized in 5% 3-aminopropyltrimethoxysilane solutions for 4 h was used according to a published procedure.[45] The aminopropylsilanated (abbreviated as APS) quartz slide was washed with water for use. The multilayer films were fabricated by immersing the APS quartz substrate alternately in $Fe_4As_4W_{30}$ and QPVP-Os solution for ~3 h. After each immersion step, the resulting films were washed with water, dried under nitrogen, and used to record UV-vis spectra to follow the deposition processes. The spectra were background subtracted using an APS quartz slide as the reference sample.

AFM. The samples were imaged with a SPA400 with an SPI-3800 controller (Seiko Instruments Industry Co., Tokyo, Japan.) at room temperature under ambient conditions. The tip type was SN-AF01 (Seiko Instruments Co.), and the cantilever used was fabricated from Si_3N_4 with a spring constant of 0.02 N m^{-1}. All images were recorded with a scan rate of about 1.0 Hz and repeated several times with different tips.

Results and discussion

Synthesis and characterization of the tetra-iron sandwich-type polyoxoanion

The compound was readily prepared in high yields and in high purity. In this procedure, several important factors were noted: (i) isomerically pure As_2W_{15} was used; (ii) the molecular ratio of Fe^{III} to As_2W_{15} was 1.5:1; (iii) reasonable pH and temperature values were adopted to avoid the formation of insoluble intermediates. In contrast to the pH observed during the synthesis of divalent sandwich compounds, the solution pH during the synthesis of tetranuclear Fe^{III} complexes remained at a very low value (pH $\sim$ 1) throughout addition of As_2W_{15}. So HCl was not added to the solution during the synthesis.

X-Ray structure of $Fe_4As_4W_{30}$. Comparison of cell parameters of $Fe_4As_4W_{30}$ with that of $Cu_4As_4W_{30}$ and the phosphorus analogs is shown in Table 1. It is clearly seen that $Fe_4As_4W_{30}$ has a similar structure to that of the $M_4X_4W_{30}$ (X = P, M = Fe, Co, Ni, Cu, Zn, Cd, Mn; X = As, M = Co, Co, Ni, Cu, Zn, Cd, Mn) series. The anion consists of two trivacant Dawson units, $As_2W_{15}O_{56}^{12-}$, linked by a Fe unit in a centrosymmetric arrangement (C_{2h} symmetry). $As_2W_{15}O_{56}^{12-}$ anion provides seven oxygen donor atoms (one from the central AsO_4 group and the other six oxygen atoms from the six WO_6 groups) that are capable of coordinating the central tetrameric metal unit to form a sandwich polyoxoanion. The four Fe atoms lie in the same plane and form a regular rhomb-like cluster. The two water molecules are coordinated to the Fe atoms. The structure of $Fe_4As_4W_{30}$ was further well characterized by means of IR, UV, and ^{183}W NMR.

IR spectra. The IR spectrum of $Fe_4As_4W_{30}$ is shown in Fig. 1 and is compared with those of $Mn_4As_4W_{30}$ and the parent anion α-As_2W_{15}. The following points can be drawn: (i) all of the characteristic vibrational frequencies including terminal W–O, bridging W–O–W and As–O stretching bands, located in the 1000–700 cm^{-1} range, occur at lower wavenumbers for the $M_4As_4W_{30}$ than for the parent saturated α-As_2W_{18} anion, which is attributed to the increase of negative charge of the anions;[46] (ii) the asymmetric stretching vibration of W–O_c–W in As_2W_{15} has 3 peaks, but only 2 peaks when $M_4As_4W_{30}$ is formed; (iii) the IR spectrum for $Fe_4As_4W_{30}$ is similar to that of $M_4As_4W_{30}$, which indicates a structural similarity throughout the entire $M_4As_4W_{30}$ series.[34]

UV spectrum. The UV spectrum of $Fe_4As_4W_{30}$, shown in Fig. 2, has two absorption bands. The higher energy band at *ca.* 200 nm is attributed to the charge transfer of $O_d \rightarrow W$ (O_d represents the terminal oxygen atoms), and the lower energy band at *ca.* 260 nm is attributed to that of (O_c/O_b) $\rightarrow$ W (O_c represents oxygen atoms coordinated to the W atoms whose octahedra are side-shared, O_b represents oxygen atoms coordinated to the W atoms whose octahedra are corner-shared), indicating that the electronic structure is similar to that of $M_4As_4W_{30}$.[34,47]

^{183}W NMR spectrum. Fig. 3 shows the ^{183}W NMR spectrum of $Fe_4As_4W_{30}$ in D_2O, which confirms its structure. Thus, eight resonances were observed at room temperature (referenced to Na_2WO_4) at −118.2, −127.9, −132.7, −136.4, −140.3, −184.2, −191.1, and −199.3 ppm, while the dimeric molecular formula requires a C_{2h} symmetry structure as shown in Fig. 4 with the eight types of tungsten atoms labeled as a_1, a_2, a_3, b_1, b_2, b_3, c_1 and c_2.[22,34]

Electrochemical behavior of $Fe_4As_4W_{30}$ and growth as a monolayer

Electrochemical behavior in solution. The electrochemical behavior of $Fe_4As_4W_{30}$ in aqueous solution was investigated and is briefly described here for comparison. $Fe_4As_4W_{30}$ compound is stable in aqueous media between pH 1.5 and 6.5. Beyond this pH range, hydrolytic decomposition of the compound will occur.

Fig. 5 shows CVs of 1.0 mM $Fe_4As_4W_{30}$ at pH 4.7 with different negative potential limits. In the potential range of 0.6 to −1.0 V, CVs of $Fe_4As_4W_{30}$ on a GCE show seven main redox waves with E_f at 0.24, 0.15, −0.028, −0.14, −0.49, −0.63 and −0.82 mV, respectively, which are attributed to four one-electron iron ($Fe^{III/II}$) redox waves and three four-electron redox couples of the tungsten-oxo species. The number of electrons for each wave is evaluated by polarographic logarithmic analysis, obtained from the slope (slope = $0.059/n$, n is the number of electrons for each wave) of plots of log ($i/i_d - i$) *versus* the potential values corresponding to each polarographic wave. The experiment was performed according to the literature method.[19a]

Fig. 6 shows CVs of $Fe_4As_4W_{30}$ in pH 4.7 acetate buffers at different scan rates. The peak currents of $Fe_4As_4W_{30}$ are linearly proportional to the square root of the scan rates, taking the reduction peaks of the III, IV, VI and VII waves as representative, as shown in the inset of Fig. 6. This indicates that the redox processes are diffusion-controlled.[5,18] The ratios i_a/i_c are non-unity and the potential separations (ΔE_p) of over 56 mV (72, 68 and 70 mV for W waves, respectively) at scan rates of 9–196 mV s^{-1} suggest a quasi-reversibility for the W waves (V, VI and VII in Fig. 6). However, the four ΔE_ps of Fe are 48, 55, 53 and 54 mV, respectively, and the ratios i_a/i_c are almost unity at the scan rates of 9–196 mV s^{-1}, as shown in Fig. 6. So the four Fe waves (I, II, III and IV in Fig. 6) can be regarded as reversible.

Although the electrochemical characterization of a tetraferric sandwich-type tungstoarsenate is lacking in the literature, Song,[19a] Anderson[32] and Ruhlmann[19b] and co-workers reported the electrochemical behavior of tetraferric sandwich-type tungstophosphate, $Fe_4P_4W_{30}$, in solution. Song and co-workers reported that the CV of $Fe_4P_4W_{30}$ exhibits one simple one-electron reduction associated to that of iron,

Table 1 Cell parameters of $Fe_4As_4W_{30}$, $Cu_4As_4W_{30}$[34] and $M_4P_4W_{30}$ (M = Fe,[32a] Cu[24c] and Mn,[27a])

Anion	$Fe_4As_4W_{30}$	$Cu_4As_4W_{30}$	$Fe_4P_4W_{30}$	$Cu_4P_4W_{30}$	$Mn_4P_4W_{30}$
Crystal system	Triclinic	Triclinic	Triclinic	Triclinic	Triclinic
Space group	$P\bar{1}$	$P\bar{1}$	$P\bar{1}$	$P\bar{1}$	$P\bar{1}$
a/Å	15.16(3)	12.72(3)	12.58(1)	13.40(9)	14.31(3)
b/Å	17.19(7)	24.52(5)	15.95(2)	25.02(13)	14.68(4)
c/Å	32.23(5)	26.45(5)	19.42(2)	13.34(9)	20.36(9)
α/°	88.71	89.90	87.05(1)	104.84	83.44
β/°	83.52	77.32	83.27(1)	114.49	80.61
γ/°	91.20	89.96	75.32(1)	82.61	73.85
U/Å^3	8501.58	8048	3744.61	3933	4042
Z	2	2	1	1	1

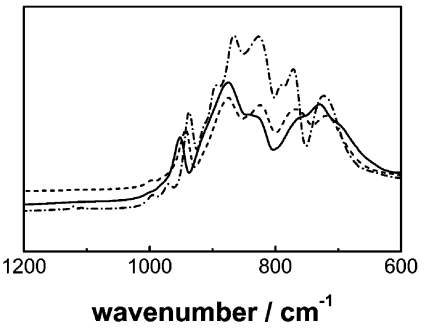

Fig. 1 IR spectra of As_2W_{15} (– · – · –), $Mn_4As_4W_{30}$ (– – –) and $Fe_4As_4W_{30}$ (—).

one four-electron reduction and one two-electron reduction associated to that of W in 0.5 M NaAc + HAc at pH 4.7;[19a] Anderson and co-workers reported that the CV of $Fe_4P_4W_{30}$ exhibits three principal unresolved reduction peaks corresponding to the $Fe^{III/II}$ redox processes, redox of tungsto-oxo is not mentioned;[32] Ruhlmann and co-workers reported that in the CV of $Fe_4P_4W_{30}$ three or four $Fe^{III/II}$ reduction waves and three four-electron W reduction waves were observed in 0.5 M $Na_2SO_4 + H_2SO_4$ at pH 2.52, but at pH > 4 the CVs become ill-defined and the peak currents much smaller.[19b] Compared with the above-mentioned results, well-defined CVs of $Fe_4As_4W_{30}$ in 0.5 M NaAc + HAc at pH 4.7 could be obtained, and the four Fe and the three W redox waves are similar to those of Ruhlmann.[19b]

Electrochemical behavior of the monolayer. Fig. 7 shows the CV of a $Fe_4As_4W_{30}$ monolayer at pH 4.7 with different negative potential limits. It exhibits six couples of redox waves with formal potentials $[(E_{pa} + E_{pc})/2]$ of 0.24, 0.059, −0.11, −0.50, −0.59, and −0.84 mV. Their ΔE_p are 45, 26, 38, 28, 30 and 64 mV, which are different from those of $Fe_4As_4W_{30}$ in solution in the same pH solution. The redox peak of $Fe^{III/II}$ at 0.24 V becomes broader because of overlapping of redox peaks I and II with the $Os(bpy)_2^{III/II}$ redox reaction of QPVP-Os occurring at the same potential.[48] The CV of QPVP-Os/4-ABA/GCE is shown in the ESI (S3). Fig. 8 shows the CV of the $Fe_4As_4W_{30}$ monolayer in pH = 4.7 acetate buffer at different scan rates. The peak currents are proportional to scan rate up to 600 mV s^{-1}, as shown in the inset of Fig. 8, taking the reduction peak of the W center as representative. This suggests that the redox reactions exhibit surface processes on the $Fe_4As_4W_{30}$/QPVP-Os/4-ABA/GCE system.[49]

The comparison of the electrochemical behavior of the $Fe_4As_4W_{30}$/QPVP-Os/4-ABA/GCE and in solution suggests that the electron-transfer processes are faster on the monolayer than in solution.

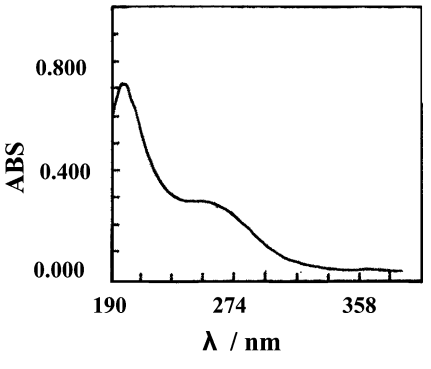

Fig. 2 UV spectrum of $Fe_4As_4W_{30}$.

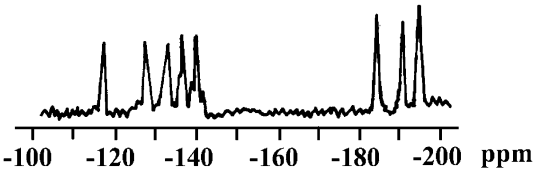

Fig. 3 ^{183}W NMR spectrum of $Fe_4As_4W_{30}$.

Layer-by-layer electrochemical growth of multilayer films consisting of $Fe_4As_4W_{30}$ and QPVP-Os

Layer-by-layer assembly based on the electrostatic attraction between polycations and polyanions was used to build up multilayer films by alternately dipping the desired substrate in QPVP-Os and $Fe_4As_4W_{30}$ solutions. After each modification CV was used to characterize the increase in quantity of modifiers loaded in the multilayer films. Fig. 9 shows the CV in pH 4.7 buffer solution in the potential region of 0.6 to −0.7 V exhibited by $n$$Fe_4As_4W_{30}$/$n$QPVP-Os/4-ABA/GCE multilayer films with $Fe_4As_4W_{30}$ as the outmost layer at different layer numbers of n = 1–9. With the number of $Fe_4As_4W_{30}$ layers increasing, the peak currents increase markedly. Taking the first reduction peak of the W center as representative, the redox peak current has a good linear relationship with the number of layers, as shown in the inset of Fig. 9. This indicates that uniform and homogeneous multilayer films have been fabricated on the 4-ABA-modified carbon substrate. Moreover, when the number of $Fe_4As_4W_{30}$ layers is larger than 9, the redox peak currents slightly increase. It is possible that $Fe_4As_4W_{30}$ deposited in the outmost layer is then so far from the electrode surface that electron transport through the films is difficult.[43]

UV-vis characterization. UV-vis spectrometry is a useful technique to characterize the growth process of multilayer films.[50] For comparison, it is helpful to refer to the UV-vis spectra of $Fe_4As_4W_{30}$ and QPVP-Os in solution. As shown in Fig. 10(A), the UV-vis spectrum of the QPVP-Os solution is characterized by two peaks with maximum absorption

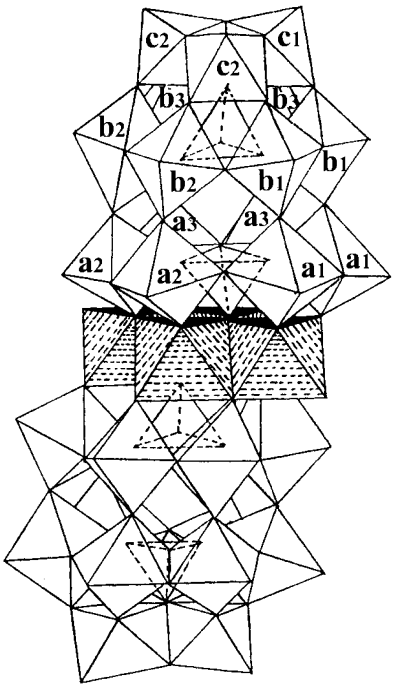

Fig. 4 Polyhedral representation of $Fe_4As_4W_{30}$.

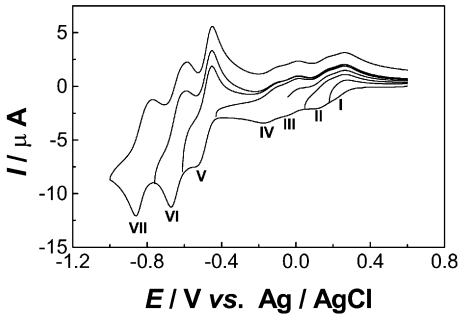

Fig. 5 CV of 1.0 mM $Fe_4As_4W_{30}$ in 0.5 M NaAc + HAc at pH 4.7 with different negative potential limits: 0.18 V, 0.048 V, −0.092 V, −0.43 V, −0.61 V, −0.76 V, and −1.0 V. Scan rate: 20 mV s^{-1}, using a GCE of 1 mm diameter as the working electrode.

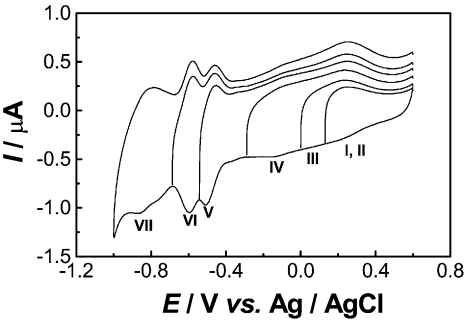

Fig. 7 CV of a monolayer CME (chemically modified electrode) of GCE/4-ABA/QPVP-Os/$Fe_4As_4W_{30}$ in NaAc + HAc buffer solutions (pH 4.7) with different negative potential limits: 0.13, 0.00, −0.29, −0.54, −0.68 and −1.0 V. Scan rate 20 mV s^{-1}.

wavelength values of 252 and 290 nm and a shoulder at ~224 nm, while that of $Fe_4As_4W_{30}$ in solution shows strong absorption near 200 nm with a weak shoulder at ~260 nm, which could be assigned to oxygen-metal charge-transfer bands.[51] The addition spectrum of the two is also given to show the possible shape of the UV-vis spectrum of the multilayer films.

Fig. 10(B) and 10(C) show the UV-vis spectra of multilayer films with $Fe_4As_4W_{30}$ as the outermost layer with different numbers of layers. In the region of 190–400 nm the UV-vis spectra of the multilayer films show three absorption shoulders that peak at approximately 200, 260, and 300 nm. The linearity of the absorption values at 200 and 260 nm *vs* the number of layers is shown in the inset of Fig. 10(B). In the region of 400–1000 nm the absorption value at *ca.* 400 nm is attributed to the $^6A_{1g} \rightarrow {}^4E_g$ transition, while the absorption value at *ca.* 500 nm is attributed to $^6A_{1g} \rightarrow {}^4T_{1g}$ of Fe(III).[51] The linearity of the absorption values at 400 nm *vs.* the number of layers is shown in the inset of Fig. 10(C). The results suggest a nearly uniform growth of the multilayer films.

XPS measurements. XPS measurements were conducted to identify the elements presented in the multilayer films. Typical XPS results for $7Fe_4As_4W_{30}$/7QPVP-Os/4-ABA/GCE are shown in Fig. 11. Two characteristic W 4f peaks and Os 4f peaks were observed at 35.5, 37.5 eV [Fig. 11(A)] and at 50.9, 52.5 eV [Fig. 11(B)], respectively, which is consistent with the previous results.[44] The As 3d and Fe 2p peaks were also found at 45.2 and 712.5 eV, respectively. This confirms that QPVP-Os and $Fe_4As_4W_{30}$ were incorporated on the GCE surface in the preparation of the multilayer films. Therefore, the presence of $Fe_4As_4W_{30}$ and QPVP-Os in the multilayer films has been confirmed by the XPS data.

Effect of pH on the electrochemical behaviour of the $Fe_4As_4W_{30}$ multilayer films. Fig. 12 shows the pH effect on the three redox peak potentials of multilayer films containing nine $Fe_4As_4W_{30}$ layers. It can be seen that the one-electron couple of Fe^{III}/Fe^{II} (line I) is less dependent on pH, while the other two redox couples of the W center shift negatively with increasing pH (lines II and III). The average slopes of the E_f *versus* pH lines for the second and third reduction peak of the W center are −67 and −69 mV per pH, corresponding to four $1e^-/1H^+$. It is confirmed that in the multilayer film, the one-electron process of Fe^{III}/Fe^{II} has no proton participation, but the two four-electron processes are accompanied by four-proton participations. The uptake of protons during the $Fe_4As_4W_{30}$ reduction avoids the charge concentration in $Fe_4As_4W_{30}$, which is commonly found for POMs.[52]

According to the above results, the redox processes of $Fe_4As_4W_{30}$ incorporated into multilayer films can be described as follows:

$$[Fe_4^{III}As_4W_{30}]^{12-} + e^- \Leftrightarrow [Fe_3^{III}Fe^{II}As_4W_{30}]^{13-}$$

$$[Fe_3^{III}Fe^{II}As_4W_{30}]^{13-} + e^- \Leftrightarrow [Fe_2^{III}Fe_2^{II}As_4W_{30}]^{14-}$$

$$[Fe_2^{III}Fe_2^{II}As_4W_{30}]^{14-} + e^- \Leftrightarrow [Fe^{III}Fe_3^{II}As_4W_{30}]^{15-}$$

$$[Fe^{III}Fe_3^{II}As_4W_{30}]^{15-} + e^- \Leftrightarrow [Fe_4^{II}As_4W_{30}]^{16-}$$

$$[Fe_4^{II}As_4W_{30}{}^{VI}]^{16-} + 4e^- + 4H^+ \Leftrightarrow [H_4Fe_4^{II}As_4W_{26}{}^{VI}W_4{}^{V}]^{16-}$$

$$[H_4Fe_4^{II}As_4W_{26}{}^{VI}W_4{}^{V}]^{16-} + 4e^- + 4H^+ \Leftrightarrow [H_8Fe_4^{II}As_4W_{22}{}^{VI}W_8{}^{V}]^{16-}$$

$$[H_8Fe_4^{II}As_4W_{22}{}^{VI}W_8{}^{V}]^{16-} + 4e^- + 4H^+ \Leftrightarrow [H_{12}Fe_4^{II}As_4W_{18}{}^{VI}W_{12}{}^{V}]^{16-}$$

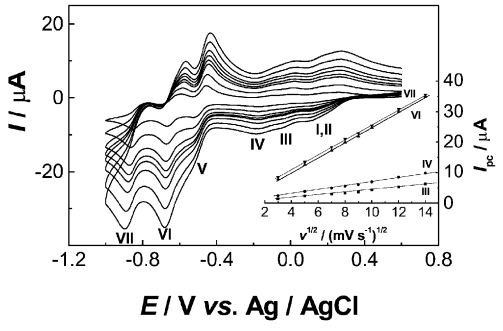

Fig. 6 CV of 1.0 mM $Fe_4As_4W_{30}$ in pH 4.7 buffer solutions at scan rates of 9, 25, 49, 64, 81, 100, 144 and 196 mV s^{-1}. The inset shows the relationship of the scan rate *vs.* the third, fourth, sixth and seventh reduction peak currents. A GCE with 1 mm diameter was used as the working electrode.

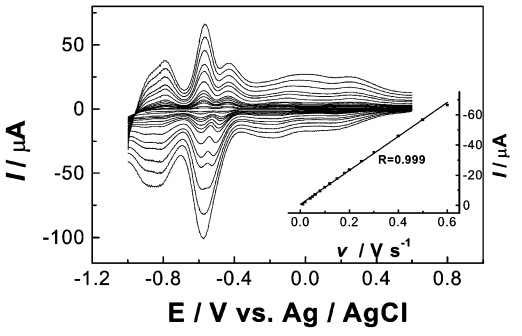

Fig. 8 CV of a monolayer CME of GCE/4-ABA/QPVP-Os/$Fe_4As_4W_{30}$ in NaAc + HAc buffer solutions (pH 4.7) at scan rates of 10, 20, 40, 60, 80, 100, 150, 200, 300, 400, 500 and 600 mV s^{-1}. The inset shows the relationship of the scan rate *vs.* the sixth reduction peak current.

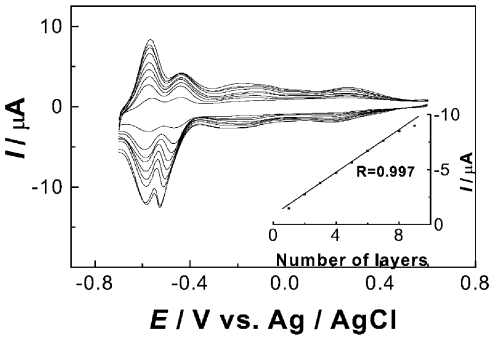

Fig. 9 CV of multilayer CMEs of GCE/4-ABA/*n*QPVP-Os/*n*$Fe_4As_4W_{30}$ in NaAc + HAc buffer solutions (pH 4.7) with increase in the number of layers *n* from 1 to 9 (shown from inside to outside curves). Scan rate: 30 mV s^{-1}. The inset shows the dependence of the second reduction peak current of the W center on the number of layers.

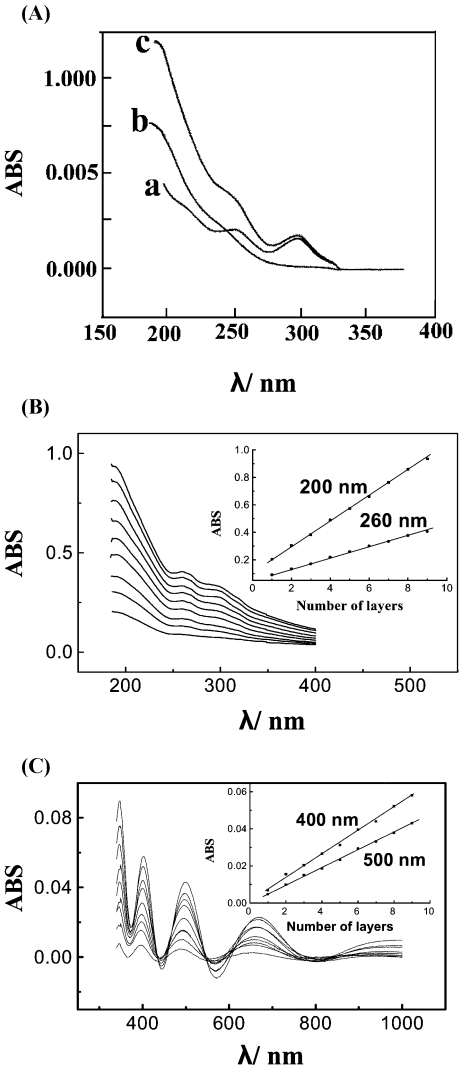

Fig. 10 (A) UV-vis spectra in pH 4.7 NaAc + HAc buffer solutions containing each of the two modifiers QPVP-Os (a) and $Fe_4As_4W_{30}$ (b) as well as an addition spectrum between the two (c). (B) and (C) UV spectra of multilayer films fabricated on a silanized quartz slide with increase in the number of outermost $Fe_4As_4W_{30}$ layers from 1 to 9 (shown from lower to upper curves). The insets show plots of the absorbance at 200, 260 nm and 400, 500 nm *vs.* the number of layers.

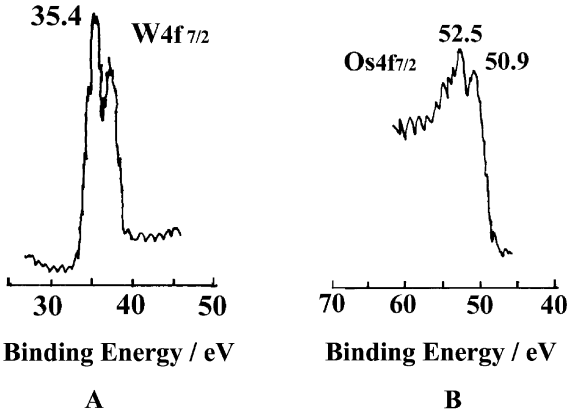

Fig. 11 XPS spectra for (A) W 4f and (B) Os 4f levels of a multilayer film: 7 $Fe_4As_4W_{30}$/7QPVP-Os/4-ABA/GCE.

On the other hand, this indicates that the multilayer films can provide a very favorable environment for electron and proton transfers that occur in the film.

Stability of the modified electrode. Stability of the 9$Fe_4As_4W_{30}$/9QPVP-Os/4-ABA/GCE multilayer films was tested by measuring the decrease of the voltammetric peak current during various experimental conditions. GCE coated with 9$Fe_4As_4W_{30}$/9QPVP-Os/4-ABA films was stored in pH 4.7 buffers and the CV measured periodically. The redox currents decrease only 1.1% after potential scanning between 0.6 and −1.0 V at 50 mV s^{-1} for about 3 h. After the multilayer film modified electrodes were exposed to air or soaked in supporting electrolyte for several months, there was only negligible change in the shape and height of the redox waves. In addition, the effect of pH on the stability of the 9$Fe_4As_4W_{30}$/9QPVP-Os/4-ABA/GCE multilayer films was also investigated. When fabricated in the multilayer films, $Fe_4As_4W_{30}$ is stable at pH 1–10. It is thus confirmed that the $Fe_4As_4W_{30}$-containing multilayer films have an excellent stability. The reason for this is mainly due to the fact that a homogeneous multilayer structure can be formed between the rigid inorganic layer of $Fe_4As_4W_{30}$ and the lithe polymeric layers of QPVP-Os, which resembles that of cross-linked polymers of high physicochemical stability.[53]

AFM measurements. AFM has been recently used as an important tool for studying films because of its unprecedented ability to give information ranging from molecular resolution crystallography to surface morphology at length scales up to about 100 μm on films with any number of layers.[54–58] Hence,

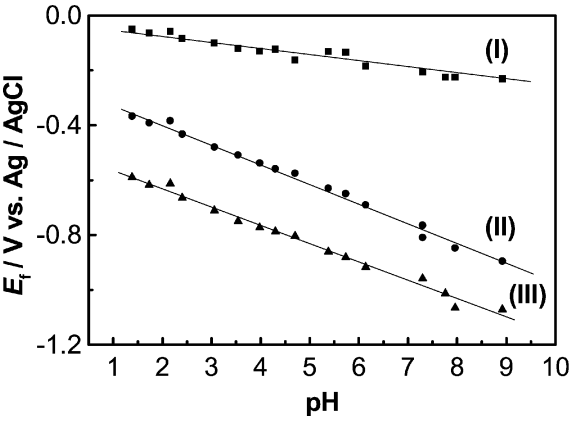

Fig. 12 Half-wave potential *vs.* pH plots for the first (I) iron redox couples and the second (II) and third (III) tungsten redox couples. Scan rate: 20 mV s^{-1}.

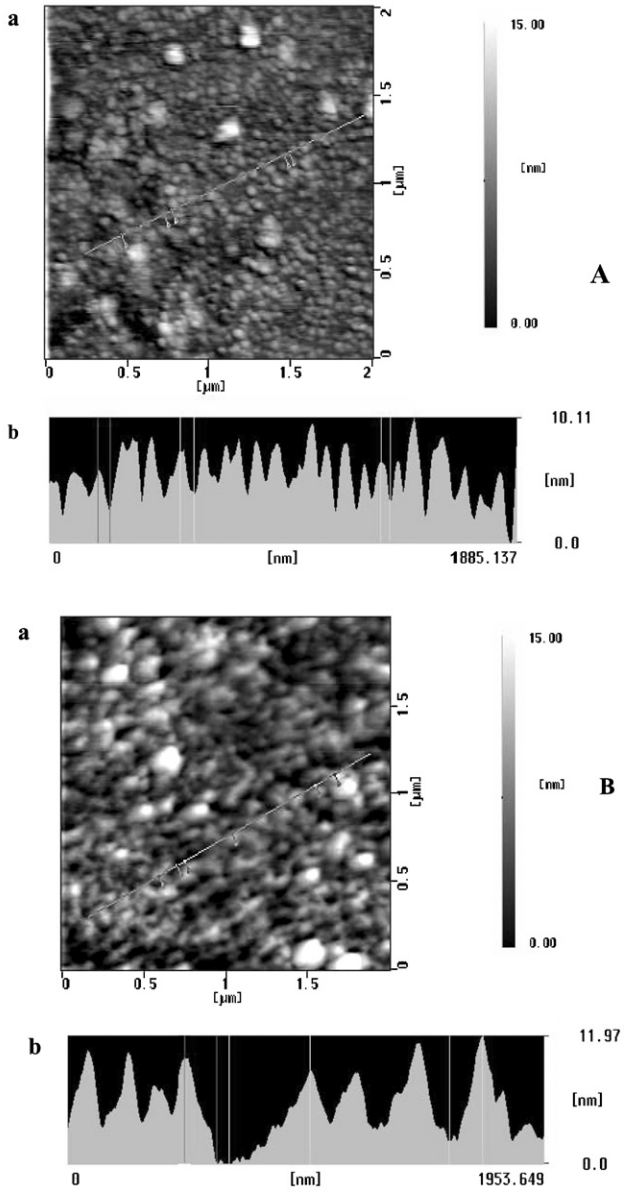

Fig. 13 AFM images of multilayer films $4Fe_4As_4W_{30}$/4QPVP-Os/4-ABA/GCE with QPVP-Os (A) and $Fe_4As_4W_{30}$ (B) as the outermost layer on ITO substrates (a). The cross-section of (a) is shown in (b).

AFM studies of $Fe_4As_4W_{30}$- QPVP-Os films can be an ideal method for checking the surface structure and defects in films. Fig. 13 shows typical AFM images of four-layer films of $Fe_4As_4W_{30}$-QPVP-Os deposited on an indium tin oxide (ITO)-coated glass slide. The four multilayer films of $(QPVP\text{-}Os)_3/(Fe_4As_4W_{30})_4$ with QPVP-Os as the outermost layer showed an AFM image with a roughness of about 1.760 nm, while $Fe_4As_4W_{30}$ as the outermost layer resulted in the formation of numerous domains with a roughness of about 3.139 nm. This indicates that the surface morphology of multilayer films with QPVP-Os as the outermost layer is significantly different from that of multilayer films with $Fe_4As_4W_{30}$ as the outermost layer. In addition, a flat surface morphology is observed over a large area (2×2 μm) and does not show any evidence for roughness of the surface or for the existence of domain structures. The homogeneity of the films suggests that the molecules deposited onto the substrate are relatively dense packing. This is important to build QPVP-Os film supermolecular assemblies with a well-defined molecular arrangement and orientation. Moreover, surface damage under a force attaining 50 nN exerted by the tip in the course of AFM imaging and reorganization of the film after aging for several days was not observed, indicating that the QPVP-Os films have a high stability.

Electrocatalytical activities of the multilayer films on the reduction of NO_2^- and H_2O_2

Because Fe(III) substituted POMs promote electrochemical reductions of some small molecules, the multilayer film modified electrode is predicted to provide heterogeneous electrocatalysis. Here, the $9Fe_4As_4W_{30}$/9QPVP-Os/4-ABA/GCE modified electrode was used in the electrocatalytic reduction of NO_2^- and H_2O_2, which are not electroactive under the same experimental conditions at a bare GCE and GCE/4-ABA/QPVP-Qs. Fig. 14(A) and 14(B) shows the CV of $9Fe_4As_4W_{30}$/9QPVP-Os/4-ABA/GCE in different solutions containing NO_2^- and H_2O_2, repectively, at various concentrations. In 0.5 M $Na_2SO_4 + H_2SO_4$ solutions (pH = 2.68), the W-centered reduction current at the potential of −0.3 V increases markedly with increasing NO_2^- concentration, while the oxidation peak decreases [Fig. 14(A)]. Apparently, the reduction of NO_2^- is effectively electrocatalyzed by $Fe_4As_4W_{30}$ incorporated in the multilayer films. The same multilayer film modified electrode exhibits a similar electrocatalytic effect on the H_2O_2 reduction in pH 5.0 buffer solutions as shown in Fig. 14(B). With the addition of H_2O_2, the cathodic current increases greatly with increasing H_2O_2 concentration at the potential of −0.2 V where Fe(III) is reduced to Fe(II), and

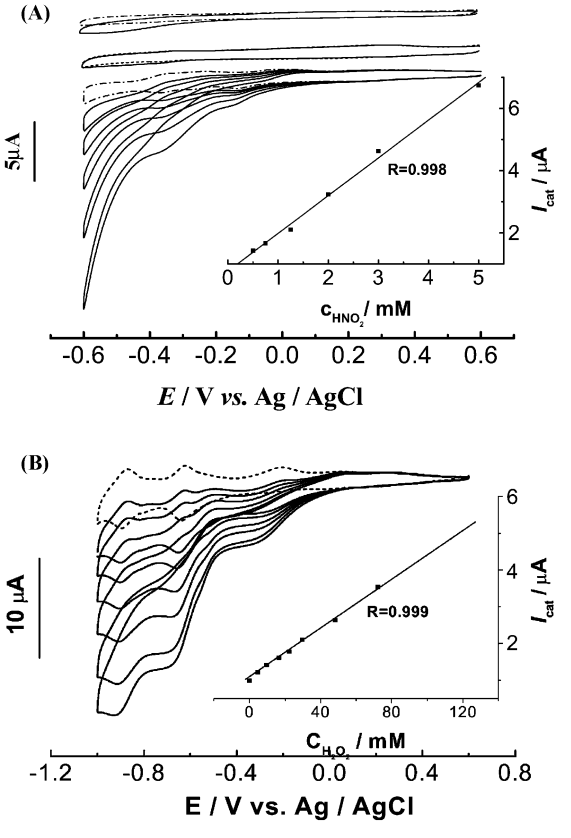

Fig. 14 (A) CV of a multilayer film of GCE/4-ABA/9QPVP-Os/$9Fe_4As_4W_{30}$ in pH 2.68 $Na_2SO_4 + H_2SO_4$ solutions containing NO_2^- at various concentrations: 0.5, 0.75, 1.25, 2, 3 and 5 mM (lower) as well as of a bare glassy carbon electrode (upper) and of GCE/4-ABA/QPVP-Qs (middle), before (---) and after (—) addition of NO_2^-. Scan rate: 20 mV s^{-1}. The inset shows relationship between catalytic current and concentration of NO_2^-. (B) CV of a multilayer film of GCE/4-ABA/9QPVP-Os/$9Fe_4As_4W_{30}$ in pH 5.0 buffer solutions containing H_2O_2 at various concentrations: 4.8, 9.6, 16.8, 22.5, 29.8, 48.2 and 72.4 mM, before (---) and after (—) addition of H_2O_2. Scan rate: 20 mV s^{-1}. The inset shows relationship between catalytic current and concentration of H_2O_2.

the corresponding reoxidation currents of Fe(II) decrease. The same results were also obtained for the Fe(III)-substituted Keggin structure $Fe^{III}SiW_{11}O_{39}^{5-}$,[17] the Dawson structure $Fe^{III}P_2W_{17}O_{61}^{7-}$[18] and $P_2W_{15}Fe_4^{III}$.[19a] It is clear that the iron center plays an essential role in the catalytic reduction of H_2O_2. The mechanisms of the reactions of H_2O_2 with $Fe^{III}SiW_{11}O_{39}^{5-}$ and $Fe^{III}P_2W_{17}O_{61}^{7-}$ have been studied by Toth *et al.*[17] and by Dong and Liu,[18] respectively. Insets in the two parts of Fig. 14 show the linear relationships between catalytic currents and corresponding concentrations of the two target substrates. Two straight lines are present over a wide range of concentrations, suggesting that the $Fe_4As_4W_{30}$-containing multilayer films will have potential applications in detection of NO_2^- and H_2O_2.

Summary

A novel compound, $Fe_4As_4W_{30}$, with potential applications in the areas of catalysis,[28a] materials[30] and medicine[33] has been synthesized. IR, UV, ^{183}W NMR and elemental analyses have been used to characterize its structure, prepared by coordination of trivacant anions of α-As_2W_{15} with four Fe(III) cations. The redox electrochemistry of $Fe_4As_4W_{30}$ has been studied in buffer solutions for the first time. The $Fe_4As_4W_{30}$ anion exhibits four one-electron Fe-based waves followed by three four-electron redox waves attributed to tungsten-oxo redox processes in pH 4.7 buffer solution. The third, fourth, sixth and seventh cathodic peak currents are almost proportional to the square root of the scan rate up to 196 mVs^{-1}, which indicates that the electrode processes of $Fe_4As_4W_{30}$ are diffusion-controlled.

The self-assembly technique has been used for controlled fabrication of well-defined monolayer and multilayer films containing $Fe_4As_4W_{30}$ on glassy carbon electrodes covered with 4-ABA. 4-ABA is covalently grafted to the GCE surface by the amino cation radical method, which makes the GCE surface negatively charged under proper pH conditions. $Fe_4As_4W_{30}$ and QPVP-Os can be strongly adsorbed alternately onto the negatively charged 4-ABA precursor. The composition, uniformity and structure of the resulting multilayer films have been characterized by CV, XPS, UV-vis and AFM. The present work demonstrates the successful preparation of composite multilayer films consisting of $Fe_4As_4W_{30}$ and QPVP-Os through layer-by-layer electrostatic deposition on a 4-ABA coated GCE surface. The $Fe_4As_4W_{30}$-containing multilayer films exhibit remarkable electrocatalytic activities for the reduction of NO_2^- and H_2O_2.

Acknowledgements

This work is supported by the National Science Foundation of China (No. 20075028 and 20275036) and China Postdoctoral Science Foundation of Baccy Head Office.

References

1 (*a*) S. Zhang, G. Huang, M. Shao and Y. Tang, *J. Chem. Soc., Chem. Commun.*, 1993, 37; (*b*) I. A. Weinstock, *Chem. Rev.*, 1998, **98**, 113; (*c*) J. F. Kirby and L. C. W. Baker, *Inorg. Chem.*, 1998, **37**, 5537; (*d*) V. A. Grigoriev, C. L. Hill and I. A. Weinstock, *J. Am. Chem. Soc.*, 2000, **122**, 3544; (*e*) V. A. Grigoriev, D. Cheng, C. L. Hill and I. A. Weinstock, *J. Am. Chem. Soc.*, 2001, **123**, 5292.
2 A. Müller, E. Krickemeyer, S. Dillinger, H. Bögge, W. Plass, A. Proust, L. Dioczik, C. Menka, J. Meyer and R. Z. Rohlfing, *Anorg. Allg. Chem.*, 1994, **620**, 599.
3 (*a*) M. T. Pope and A. Müller, *Angew. Chem.*, 1991, **103**, 56; (*b*) M. T. Pope and A. Müller, *Angew. Chem., Int. Ed. Engl.*, 1991, **30**, 34; (*c*) V. W. Day, W. G. Klemperer and D. J. Maltbie, *J. Am. Chem. Soc.*, 1987, **109**, 2991.
4 (*a*) L. Ouahab, *Chem. Mater.*, 1997, **9**, 1909; (*b*) A. Müller, F. Peters, M. T. Pope and D. Gatteschi, *Chem. Rev.*, 1998, **98**, 239; (*c*) A. Müller, S. K. Das, P. Kogerler, H. Bogge, M. Schmidtmann, A. X. Trautwein, V. Schunemann, E. Krickmeyer and W. Preetz, *Angew. Chem., Int. Ed.*, 2000, **39**, 3414 and references therein; (*d*) E. Coronado and C. J. Gomez-García, *Chem. Rev.*, 1998, **98**, 273; (*e*) J. M. Clemente-Juan and E. Coronado, *Coord. Chem. Rev.*, 1999, **193–195**, 361.
5 (*a*) X. D. Xi, G. Wang, B. F. Liu and S. J. Dong, *Electrochim. Acta.*, 1995, **40**, 1025; (*b*) M. Kozik and L. C. W. Baker, *J. Am. Chem. Soc.*, 1990, **112**, 7604.
6 (*a*) L. H. Bi, Q. Z. He, Q. Jia and E. B. Wang, *J. Mol. Struct.*, 2001, **597**, 83; (*b*) L. H. Bi, E. B. Wang, L. Xu and R. D. Huang, *Inorg. Chim. Acta.*, 2000, **305**, 163.
7 (*a*) B. Keita and L. Nadjo, *J. Electroanal. Chem.*, 1987, **227**, 77; (*b*) B. Keita and L. Nadjo, *J. Electroanal. Chem.*, 1988, **247**, 157; (*c*) B. Keit, A. Belhouari, L. Nadjo and R. Contant, *J. Electroanal. Chem.*, 1995, **181**, 243; (*d*) J. E. Toth and F. C. Anson, *J. Am. Chem. Soc.*, 1989, **111**, 2444.
8 (*a*) B. Wang and S. Dong, *J. Electroanal. Chem.*, 1992, **245**, 328; (*b*) B. Wang, F. Song and S. Dong, *J. Electroanal. Chem.*, 1993, **353**, 43; (*c*) S. Dong, X. D. Xi and M. Tian, *J. Electroanal. Chem.*, 1995, **385**, 227; (*d*) S. Dong and Z. Jin, *J. Chem. Soc., Chem. Commun.*, 1987, 1871.
9 (*a*) L. H. Bi, R. D. Huang and E. B. Wang, *J. Chem. Soc., Dalton Trans.*, 2001, 121; (*b*) M. Sadakane, M. H. Dickman and M. T. Pope, *Inorg. Chem.*, 2001, **40**, 2715; (*c*) K. Wassermann and M. T. Pope, *Inorg. Chem.*, 2001, **40**, 2763.
10 C. L. Hill and C. M. Prosser-McCartha, *Coord. Chem. Rev.*, 1995, **143**, 407.
11 M. Sadakane and E. Steckhan, *J. Mol. Catal., A*, 1996, **114**, 221.
12 (*a*) C. Rong and M. T. Pope, *J. Am. Chem. Soc.*, 1992, **114**, 2932; (*b*) C. Rong and F. C. Anson, *Inorg. Chem.*, 1994, **33**, 1064.
13 (*a*) J. C. Bart and F. C. Anson, *J. Electroanal. Chem.*, 1995, **390**, 11; (*b*) B. Keita, Y. W. Lu, L. Nadjo, R. Contant, M. Abbessi, J. Canny and M. Richet, *J. Electroanal. Chem.*, 1999, **477**, 146; (*c*) B. Keita, F. Girard, L. Nadjo, R. Contant, J. Canny and M. Richet, *J. Electroanal. Chem.*, 1999, **478**, 76; (*d*) B. Keita, K. Essaadi, L. Nadjo, R. Contant and Y. J. Justum, *J. Electroanal. Chem.*, 1996, **404**, 271.
14 (*a*) N. I. Kuznetsova, L. I. Kuznetsova and V. A. Likholobov, *J. Mol. Catal.*, 1996, **108**, 135; (*b*) X. Zhang, K. Sasaki and C. L. Hill, *J. Am. Chem. Soc.*, 1996, **118**, 4809; (*c*) J. B. Tommasino, R. Contant, J. P. Michaut and J. Roncin, *Polyhedron*, 1998, **17**, 357.
15 (*a*) F. Ortéga and M. T. Pope, *Inorg. Chem.*, 1984, **23**, 3292; (*b*) X. Y. Zhang, M. T. Pope, M. R. Chance and G. B. Jameson, *Polyhedron*, 1995, **14**, 1381.
16 F. Zonnevijlle, C. M. Tourne and G. F. Tourne, *Inorg. Chem.*, 1982, **21**, 2751.
17 (*a*) J. E. Toth, J. D. Melton, D. Cabelli, B. H. J. Bielski and F. C. Anson, *Inorg. Chem.*, 1990, **29**, 1952; (*b*) J. E. Toth and F. C. Anson, *J. Electroanal. Chem.*, 1988, **256**, 361.
18 S. Dong and M. Liu, *J. Electroanal. Chem.*, 1994, **372**, 95.
19 (*a*) W. B. Song, X. H. Wang, Y. Liu and H. D. Xiu, *J. Electroanal. Chem.*, 1999, **476**, 85; (*b*) L. Ruhlmann, L. Nadjo, J. Canny, R. Contant and R. Thouvenot, *Eur. J. Inorg. Chem.*, 2002, 975.
20 R. G. Fink, M. Droege, J. R. Hutchinson and U. Gansow, *J. Am. Chem. Soc.*, 1981, **103**, 1587.
21 R. G. Finke and M. W. Droege, *Inorg. Chem.*, 1983, **22**, 1006.
22 R. G. Finke, M. W. Droege and P. J. Domaille, *Inorg. Chem.*, 1987, **26**, 3886.
23 R. Finke and T. J. R. Weakley, *J. Chem. Crystallogr.*, 1994, **24**, 123.
24 (*a*) T. J. R. Weakley, H. T. Evans, J. S. Showell, G. F. Tourné and C. M. Tourné, *J. Chem. Soc., Chem. Commun.*, 1973, 139; (*b*) H. T. Evans, C. M. Tourné, G. F. Tourné and T. J. R. Weakley, *J. Chem. Soc., Dalton Trans.*, 1986, 2699; (*c*) T. J. R. Weakley and R. G. Finke, *Inorg. Chem.*, 1990, **29**, 1235.
25 (*a*) K. C. Kim and M. T. Pope, *J. Am. Chem. Soc.*, 1999, **121**, 8512; (*b*) X. Y. Zhang, G. B. Jameson, C. J. O'Connor and M. T. Pope, *Polyhedron*, 1996, **15**, 2934.
26 E. Coronado and C. J. Gómez-García, *Comments Inorg. Chem.*, 1995, **17**, 255.
27 (*a*) C. J. Gomez-Garcia, J. J. Borras-Almenar, E. Coronado and L. Ouahab, *Inorg. Chem.*, 1994, **33**, 4016; (*b*) J. M. Clement-Juan, E. Cironado, J. R. Galan-Mascaros and C. J. Gomez-García, *Inorg. Chem.*, 1999, **38**, 55.
28 (*a*) X. Zhang, Q. Chen, D. C. Duncan, R. J. Lachicotte and C. L. Hill, *Inorg. Chem.*, 1997, **36**, 4381; (*b*) J. T. Rhule, C. L. Hill and

D. A. Judd and *Chem. Rev.*, 1998, **98**, 327.(*c*) X. Zhang, T. M. Anderson, Q. Chen and C. L. Hill, *Inorg. Chem.*, 2001, **40**, 418.
29 R. Neumann, *Prog. Inorg. Chem.*, 1998, **47**, 317.
30 (*a*) U. Kortz, S. Isber, M. H. Dickman and D. Ravot, *Inorg. Chem.*, 2000, **39**, 2915; (*b*) C. Craciun, L. David, D. Rusu, M. Rusu, O. Cozar and G. Marcu, *J. Radioanal. Nucl. Chem.*, 2001, **247**, 307.
31 (*a*) C. J. Gomez-Garcia, N. Casan-Pastor, E. Coronado, L. C. W. Baker and G. Pourroy, *J. Appl. Phys.*, 1990, **67**, 5995; (*b*) C. J. Gomez-Garcia, E. Coronado and J. J. Borras-Almenar, *Inorg. Chem.*, 1992, **31**, 1667; (*c*) C. J. Gomez-Garcia, E. Coronado, P. Comez-Romero and N. Casan-Pastor, *Inorg. Chem.*, 1993, **32**, 3378; (*d*) N. Casan-Pastor, E. Coronado, G. Pourroy and L. C. W. Baker, *J. Am. Chem. Soc.*, 1992, **114**, 10 380; (*e*) C. J. Gomez-Garcia, E. Coronado, J. J. Borras-Almenar, M. Aebersold, H. U. Gudel and H. Mutka, *Phys. B*, 1992, **180–181**, 238; (*f*) J. M. Clemente-Juan, H. Andres, M. Aebersdd, J. J. Borrás-Almenar, E. Coronado, H. U. Güdel, G. Kearley and H. Büttner, *Inorg. Chem.*, 1997, **36**, 2244; (*g*) J. M. Clemente-Juan, H. Andres, J. J. Borrás-Almenar, E. Coronado, H. U. Güdel, M. Aebersold, G. Kearly, H. Büttner and M. Zolliker, *J. Am. Chem. Soc.*, 1999, **121**, 10 021; (*h*) H. Andres, J. M. Clemente-Juan, M. Aebersild, H. U. Güdel, E. Coronado, H. Büttner, G. Kearly, J. Melero and R. Burried, *J. Am. Chem. Soc.*, 1999, **121**, 10 028; (*i*) J. M. Clemente-Juan, E. Coronado, J. R. Galán-Masoarós and C. J. Gómez-García, *Inorg. Chem.*, 1999, **38**, 55.
32 (*a*) X. Zhang, Q. Chen, D. C. Duncan, C. F. Campana and C. L. Hill, *Inorg. Chem.*, 1997, **36**, 4208; (*b*) A. M. Khenkin and C. L. Hill, *Mendeleev Commun.*, 1993, 140.
33 D. A. Judd, R. F. Schinazi and C. L. Hill, *Antiviral Chem. Chemother.*, 1994, **5**, 410.
34 L. H. Bi, E. B. Wang, J. Peng and R. D. Huang, *Inorg. Chem.*, 2000, **39**, 671.
35 (*a*) A. Kuhn, N. Mano and C. Vidal, *J. Electroanal. Chem.*, 1999, **462**, 187; (*b*) F. Caruso, D. G. Kurth, D. Volkmer, M. J. Koop and A. Müler, *Langmuir*, 1998, **14**, 3462; (*c*) I. Ichinose, H. Tagawa, S. Mizuki, Y. Lvov and T. Kunitake, *Langmuir*, 1998, **14**, 187; (*d*) A. J. Downard and A. Mohamed, *Electroanalysis*, 1999, **11**, 418; (*e*) H. Tanaka and A. Aramata, *J. Electroanal. Chem.*, 1997, **437**, 29; (*f*) R. S. Deinhammer, M. Ho, J. W. Anderegg and M. D. Porter, *Langmuir*, 1994, **10**, 1306.
36 L. Cheng, L. Niu, J. Gong and S. J. Dong, *Chem. Mater.*, 1999, **11**, 1465.
37 (*a*) B. Barbier, J. Pinson, G. Desarmot and M. Sanchez, *J. Electrochem. Soc.*, 1990, **137**, 1757; (*b*) L. Cheng, J. Liu and S. Dong, *Anal. Chim. Acta.*, 2000, **417**, 133; (*c*) J. Liu and S. Dong, *Electrochem. Commun.*, 2000, **2**, 707.
38 (*a*) P. Allongue, M. Delamar, B. Desbat, O. Fagebarme, R. Hitmi, J. Pinson and J. M. Saveant, *J. Am. Chem. Soc.*, 1997, **119**, 201; (*b*) S. Dong, L. Cheng and X. Zhang, *Electrochim. Acta.*, 1998, **43**, 563; (*c*) L. Cheng, X. Zhang, X. Xi, B. Liu and S. Dong, *J. Electroanal. Chem.*, 1996, **407**, 97; (*d*) S. Dong and B. Wang, *Electrochim. Acta.*, 1992, **37**, 11; (*e*) B. Wang and S. Dong, *Electrochim. Acta.*, 1993, **38**, 1029.
39 M. Delamar, R. Hitmi, J. Pinson and J. M. Saveant, *J. Am. Chem. Soc.*, 1992, **114**, 5883.
40 (*a*) G. Bidan, E. M. Genies and M. Lapkowski, *J. Electroanal. Chem.*, 1988, **251**, 297; (*b*) G. Bidan, E. M. Genies and M. Lapkowski, *J. Chem. Soc., Chem. Commun.*, 1988, **533**; (*c*) G. Bidan, M. Lapkowski and J. P. Travers, *Synth. Met.*, 1989, **28**, C113; (*d*) G. Bidan, E. M. Genies and M. Lapkowski, *J. Electroanal. Chem.*, 1988, **255**, 303; (*e*) L. Cheng and S. Dong, *Electrochem. Commun.*, 1999, **1**, 159; (*f*) C. Moiroux and J. Pinson, *J. Electroanal. Chem.*, 1992, **336**, 113; (*g*) S. Dong and W. Jin, *J. Electroanal. Chem.*, 1993, **354**, 87; (*h*) S. Dong and M. Liu, *J. Electroanal. Chem.*, 1994, **372**, 95; (*i*) M. Liu and S. Dong, *Electrochim. Acta.*, 1995, **40**, 197; (*j*) B. Keita, A. Belhouari and L. Nadjo, *J. Electroanal. Chem.*, 1993, **355**, 235; (*k*) B. Keita, N. Dellero and L. Nadjo, *J. Electroanal. Chem.*, 1991, **302**, 47; (*l*) A. Papadakis, A. Souliotis and E. Papaconstantinou, *J. Electroanal. Chem.*, 1997, **435**, 17; (*m*) A. M. Bond, J. B. Coopera, F. Marken and D. M. Way, *J. Electroanal. Chem.*, 1995, **396**, 407.
41 (*a*) M. Clemente-León, E. Coronado, P. Delhaes, C. J. Gómez-García and C. Mlngotaud, *Adv. Mater.*, 2001, **13**, 574; (*b*) J. M. Clemente-León, E. Coronado, J. R. Galán-Mascarós, O. Giménez-Salz, C. J. Gómez-García and T. F. Otero, *J. Mater. Chem.*, 1998, **8**, 309.
42 L. H. Bi, J. Y. Liu, Y. Shen, J. G. Jiang, E. K. Wang and S. J. Dong, *Chem. J. Chin. Univ.*, 2002, **23**, 472.
43 J. Liu, L. Cheng, B. Liu and S. Dong, *Electroanalysis*, 2001, **13**, 993.
44 J. Y. Liu, L. Cheng, B. F. Liu and S. J. Dong, *Langmuir*, 2000, **16**, 7471.
45 (*a*) I. Haller, *J. Am. Chem. Soc.*, 1978, **100**, 8050; (*b*) F. Pintchorski, J. B. Price, P. J. Tobin, J. Peavey and D. Kobold, *J. Electrochem. Soc.*, 1987, **134**, 3559.
46 R. Contant and R. Thouvenot, *Can. J. Chem.*, 1991, **69**, 1498.
47 (*a*) H. T. Evans and B. M. Gatehouse, *J. Chem. Soc., Dalton Trans.*, 1975, 505; (*b*) L. H. Bi, J. Peng, Y. G. Chen and L. Y. Qu, *Polyhedron*, 1994, **13**, 2421.
48 A. Kuhn and F. C. Anson, *Langmuir*, 1996, **12**, 5481.
49 R. W. Murray, in *Electroanalytical Chemistry*, ed. A. J. Bard, Marcel Dekker, New Yok, 1984, vol. 13, p. 191.
50 (*a*) M. Ferreira and M. F. Rubner, *Macromolecules*, 1995, **28**, 7170; (*b*) K. Araki, W. M. J. Wagner and M. S. Wrighton, *Langmuir*, 1996, **12**, 5393; (*c*) X. Zhang, M. Gao, X. Kong, Y. Sun and J. Shen, *J. Chem. Soc., Chem. Commun.*, 1994, 1055; (*d*) C. Sun and J. Zhang, *Electroanalysis*, 1997, **9**, 1365; (*e*) C. Sun and J. Zhang, *Electrochim. Acta.*, 1998, **43**, 943.
51 (*a*) M. T. Pope, *Heteropoly and Isopoly Oxometalates*, Springer-Verlag, New York, 1983; (*b*) H. So and M. T. Pope, *Inorg. Chem.*, 1972, **11**, 1441.
52 (*a*) L. H. Bi, E. B. Wang and R. D. Huang, *J. Mol. Struct.*, 2000, **553**, 167; (*b*) B. Keita, K. Eassadi and L. Nadjo, *J. Electroanal. Chem.*, 1989, **259**, 127; (*c*) N. Oyama and F. C. Anson, *J. Electrochem. Soc.*, 1980, **127**, 247; (*d*) B. Keita and L. Nadjo, *Mater. Chem. Phys.*, 1989, **22**, 77.
53 D. Ingersoll, P. J. Kulesza and L. R. Faulkner, *J. Electrochem. Soc.*, 1994, **141**, 140.
54 S. Liu, Z. Tang, E. Wang and S. Dong, *Thin Solid Films*, 1999, **339**, 277.
55 L. Bourdieu, P. Silberzan and D. Chatenay, *Phys, Rev. Lett.*, 1991, **67**, 2029.
56 J. P. K. Peltonen, P. He and J. B. Rosenholm, *J. Am. Chem. Soc.*, 1992, **114**, 7637.
57 J. Garnaes, D. K. Schwartz, R. Viswanathan and J. A. N. Zasadzinski, *Nature (London)*, 1992, **357**, 54.
58 D. K. Schwartz, J. Garnaes, R. Viswanathan and J. A. N. Zasadzinski, *Science*, 1992, **257**, 508.